Korean J. Chem. Eng., 32(6), 1069-1074 (2015)
DOI: 10.1007/s11814-014-0304-z

pISSN: 0256-1115
eISSN: 1975-7220

Highly stable palladium-loaded TiO_2 nanotube array electrode for the electrocatalytic hydrodehalogenation of polychlorinated biphenyls

Chunyue Cui*, Juan Wu*, Yanjun Xin*, and Yanhe Han,†**

*School of Resource and Environment, Qingdao Agricultural University, Qingdao 266109, China
**Department of Environmental Engineering, Beijing Institute of Petrochemical Technology, 19 Qingyuan North Road, Daxing District, Beijing 102617, China
(*Received 3 May 2014 • accepted 8 October 2014*)

Abstract−Palladized TiO_2 nanotube array electrode was prepared for the electrocatalytic hydrodehalogenation (HDH) of 2,4,5-trichlorobiphenyl (2,4,5-PCB). The TiO_2 nanotube array electrode was successfully fabricated by anodic oxidation method, and Pd was loaded onto the TiO_2 nanotubes by electrochemical deposition. The morphology and structure of the nanotube array electrodes with and without Pd catalysts were evaluated by scanning electron microscopy (SEM), X-ray diffraction (XRD), and X-ray photoelectron spectroscopy (XPS). The results showed that the diameters and lengths of the TiO_2 nanotubes were 30-50 nm and 200-400 nm, respectively. The particle size of the Pd was about 12 nm. Electrocatalytic HDH of 2,4,5-PCB with the Pd/TiO_2 nanotube array electrode was performed in H-cell reactor. Under a constant potential of −1.0 V, the HDH efficiency of 2,4,5-PCB was 90% and the biphenyl yield was 83% (15% current efficiency) within 180 min at the Pd/TiO_2 nanotube array electrode. Compared with the Pd/Ti electrode, the Pd/TiO_2 nanotube array electrode exhibited higher HDH efficiency and stability. Additionally, the effect of the primary HDH factors was also investigated.

Keywords: TiO_2 Nanotube, Electrocatalytic Hydrodehalogenation, Polychlorinated Biphenyls, Palladium

INTRODUCTION

Polychlorinated biphenyls (PCBs) are the most widespread pollutants in the global ecosystem and are considered persistent organic pollutants (POPs) [1,2]. It has been reported that their toxicity is related to their chlorine content [3,4]. Therefore, it is highly desirable to develop an efficient and safe technology for the dechlorination of PCBs and to convert them into potentially biodegradable products [5]. Since 1975, electrochemical dechlorination has been suggested as a promising method for the dechlorination of polyhalogenated organic waste [6]. Using this method, halogen atoms can be removed under mild experimental conditions without using toxic and reactive reducing agents [7-9].

During electrochemical dechlorination, electrodes play a very important role for achieving a high dechlorination efficiency and high current efficiencies. Mercury [10] and lead [11] were early used as the electrodes in direct electrochemical dechlorination because of their high hydrogen overvoltage. These electrode materials showed high dechlorination efficiencies, but their toxicity was not desirable from an environmental viewpoint.

Recently, indirect electrocatalytic hydrodehalogenation (HDH) has been suggested as a promising method because of its rapid reaction rate, mild reaction conditions, and the use of environmentally friendly electrodes [12]. Among the factors affecting electrocatalytic HDH, the catalyst and its supporting materials are very important. Noble metals such as Ag, Cu, and Pd with high catalytic activity are normally used as catalysts [13-16]. However, Pd has been considered as the most ideal catalyst for HDH for its unique hydrogen absorption behavior. Various materials such as titanium [17,18], nickel [19,20], and carbon materials [21,22] have been used as cathode substrates to support Pd catalysts.

The efficiency of the electrocatalytic HDH of chlorinated compounds is related to the cathode substrates, which was confirmed by the HDH of pentachlorophenol (PCP) in a 0.05 M Na_2SO_4 solution using different cathodes. More than 95% conversion of 0.071 mM PCP was achieved on a Pd/Ti mesh cathode. However, Pd/carbon cloth and Pd/Fe gauze cathodes showed lower conversion efficiencies of around 80 and 25%, respectively [23]. Our previous work [24] also reported that the electrocatalytic HDH of PCP was feasible, using palladized carbon materials as electrodes. Compared with graphite, palladized multi-walled carbon nanotubes exhibited a higher dechlorination efficiency.

However, the high prices and limited resources of palladium have hindered the practical application of electrocatalytic HDH for the dechlorination of chlorinated compounds. Currently, the reports concerning electrocatalytic HDH have mainly focused on HDH efficiency, while the stability of the electrode was little reported. Only a few studies investigated the stability of the palladium catalyst, and shown that the activity and stability of the palladium deceased sharply when an electrode of palladium was repeatedly used [24, 25]. Thus, the enhancement of catalyst activity and stability is very important for the development of electrocatalytic HDH.

TiO_2 electrode is a perfect material with high electrocatalytic activity, low resistance, and high stability [26,27]. Therefore, the Pd

†To whom correspondence should be addressed.
E-mail: hanyanhe@bipt.edu.cn, hanyanhe@126.com

catalyst-loaded TiO_2 support was used in the catalytic hydrogenation of p-nitrophenol, and exhibited higher catalytic activity and stability [28]. However, to our knowledge, no study has been published on the electrocatalytic HDH of polychlorinated biphenyls using TiO_2 nanotube array electrode.

In this study, TiO_2 nanotube array substrate was fabricated by anodic oxidation on titanium (Ti) foil. Pd was loaded onto the TiO_2 nanotube array electrode by electrochemical deposition. The Pd/TiO_2 nanotube array electrode showed high activity and stability for the electrocatalytic HDH of 2,4,5-trichlorobiphenyl (2,4,5-PCB) in an aqueous solution.

MATERIALS AND METHODS

1. Preparation of TiO_2 Nanotube Array Electrode

The TiO_2 nanotube array on a Ti substrate was fabricated by direct anodic oxidation [29]. First, a Ti plate was polished with abrasive paper and rinsed with deionized water in an ultrasonic bath for 10 min. It was then chemically etched by immersion in a mixture solution of HF and HNO_3. Finally, it was rinsed with deionized water and dried at room temperature.

Anodization was carried out in a 0.5 wt% NH_4F and 1 M $(NH_4)_2SO_4$ aqueous solution with the Ti plate as the anode and a Pt plate as the cathode. The pH of the electrolyte was adjusted to 6. Anodization with a voltage of 20 V was performed at room temperature for 2 h. Then, the sample was rinsed and dried at room temperature.

2. Electrodeposition of Pd

The palladized Ti and TiO_2 nanotube array electrode was prepared by galvanostatic electrodeposition in an aqueous solution containing 1 mM $Pd(NO_3)_2$ and 0.02 M H_2SO_4. Palladium was electrodeposited at a constant current of 1 mA/cm^2 with stirring at 30 °C. The Pd amount on the electrodes was calculated on the basis of the concentration of residual Pd ions in the solution. And the residual amount was controlled by the electro-deposition time.

3. Electrocatalytic HDH of 2,4,5-PCB

The electrocatalytic HDH of 2,4,5-PCB was carried out in a glass-made H-cell (the volume of electrolyte in each compartment was 50 mL) and the two compartments were separated by a cation exchange membrane (Nafion N324; DuPont Company, USA) (Fig. 1).

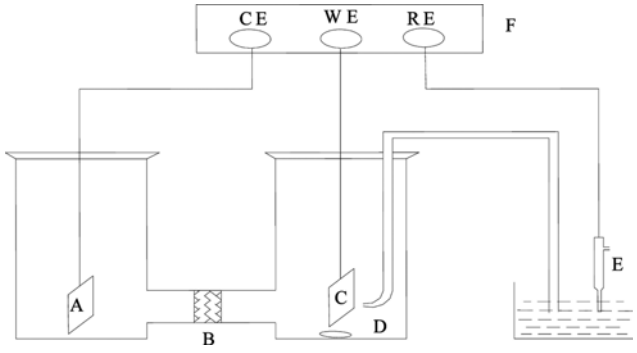

Fig. 1. Schematic diagram of the electrolytic cell. (a) Pt counter electrode; (b) cation exchange membrane; (c) Pd/TiO_2 working electrode; (d) magnetic bar; (e) reference electrode; (f) potentiostat.

The working electrode was a 6 cm^2 palladized TiO_2 nanotube array electrode, the counter electrode was a 6 cm^2 Pt plate, and the reference electrode was a saturated calomel electrode (SCE). To improve the solubility of PCBs and the conductivity of the solution, the catholyte solution consisted of a 40% methanol aqueous solution with 0.1 M hexadecyltrimethylammonium bromide (CTAB) and 0.1 M NaAc. To continuously provide H ions for the HDH reaction, the anodic compartment was filled with 0.2 M H_2SO_4 as the support electrolyte. Potentiostatic measurements were performed using a DJS-292 potentiostat (Shanghai Rex Instrument Co., China). All experiments were at room temperature (25±0.5 °C), and all potentials were reported relative to the SCE.

4. Analytical Method

The concentrations of chlorinated biphenyls and biphenyl (BP) were determined by high-performance liquid chromatography (HPLC) (PU-1580, UV-1575; Jasco, Japan) using an ultraviolet absorbance detector equipped with a Kromasil ODS column (250 mm×4.6 mm×5 μm). HPLC analyses were at room temperature at a detector wavelength of 254 nm. The mobile phase was a mixed solution containing acetonitrile : water=9 : 1 (v : v) at a flow rate of 1 mL/min.

The electrode surface morphology was characterized by scanning electron microscopy (SEM; Philips, Netherlands), X-ray diffraction (XRD; LabxXRD-6000; Shimadzu, Japan), and X-ray photoelectron spectroscopy (XPS; PHI-5000, USA). Pd was analyzed by ICP-AES (Advantage; IRIS, USA).

5. Determination of the Current Efficiency

The HDH current efficiency was calculated as the part of the current (average current at constant voltage) that was used to convert the 2,4,5-PCBs ($Cl_3C_{12}H_7$) reactant to the intermediates and the product:

Intermediate formation: $Cl_3C_{12}H_7+2e^-+H^+\rightarrow Cl_2C_{12}H_8+Cl^-$ (1)

$Cl_3C_{12}H_7+4e^-+2H^+\rightarrow ClC_{12}H_9+2Cl^-$ (2)

Product formation: $Cl_3C_{12}H_7+6e^-+3H^+\rightarrow C_{12}H_{10}+3Cl^-$ (3)

Therefore, the current efficiency (φ) for the production of $Cl_2C_{12}H_8$, $ClC_{12}H_9$, and $C_{12}H_{10}$ from $Cl_3C_{12}H_7$, is defined as [8]:

$$\varphi=\varphi_1+\varphi_2+\varphi_3 \quad (4)$$

where φ_1, φ_2, and φ_3 are the current efficiencies for the formation of $Cl_2C_{12}H_8$, $ClC_{12}H_9$, and $C_{12}H_{10}$, respectively. These intermediates and product were calculated using quantitative HPLC data and the charge that passed.

RESULTS AND DISCUSSION

1. Characterization of Electrodes

The SEM images of the electrodes are shown in Fig. 2. Fig. 2(a) and (b) show the SEM images for Ti and the TiO_2 nanotube array electrode. Fig. 2(b) shows that the TiO_2 nanotubes are well aligned and organized into regular uniform arrays. The diameters of the tubes are about 30-50 nm and their lengths are about 200-400 nm. SEM images of the Pd/Ti and Pd/TiO_2 nanotube array electrodes with the same amount of Pd (1.8 mg/cm^2) are shown in Fig. 2(c) and Fig. 2(d), respectively. The results show that the Pd particles on the TiO_2 nanotube array electrode are more uniformly dispersed than those on the Ti electrode with a small particle size. This is prob-

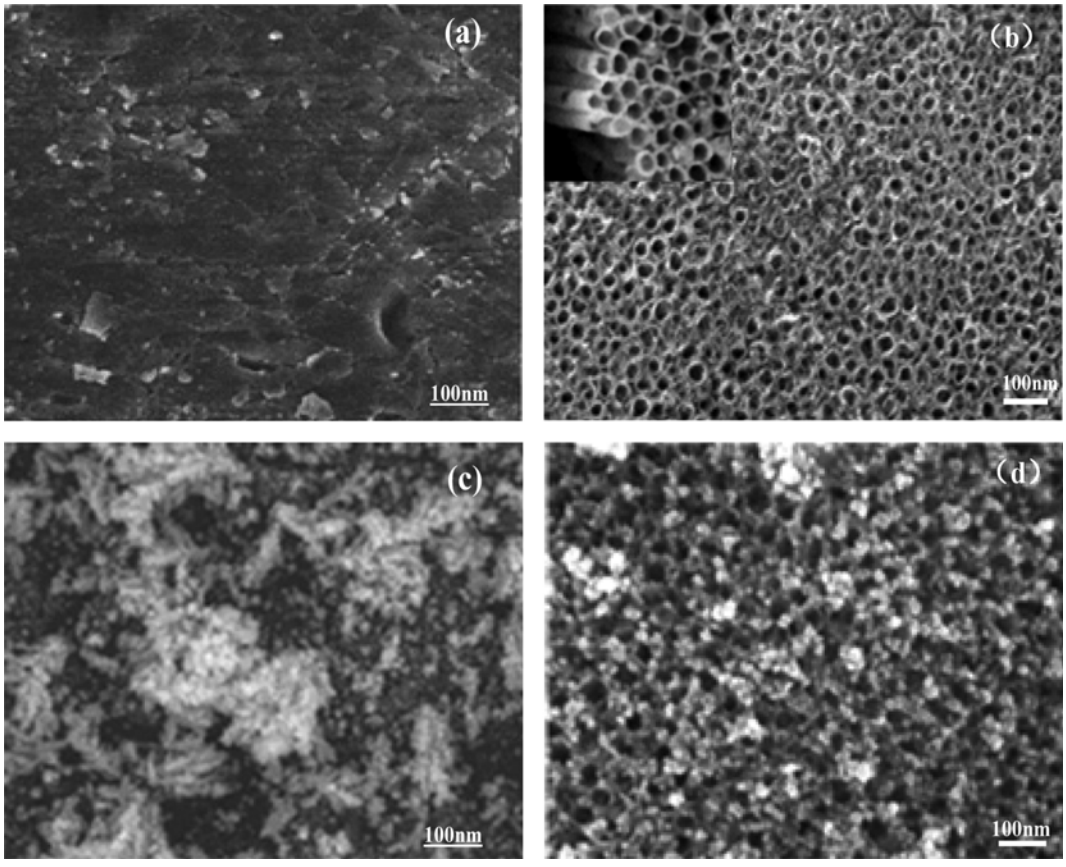

Fig. 2. SEM images of (a) Ti; (b) the TiO_2 nanotube array; (c) Pd/Ti; and (d) the Pd/TiO_2 nanotube array electrodes.

ably because of the effect of the three-dimensional structure of the TiO_2 nanotube array on Pd deposition.

XRD patterns of the TiO_2 and Pd/TiO_2 nanotube array electrode are shown in Fig. 3. The dispersion peak at 15-25° corresponds to the amorphous alloy TiO_2 and the peaks at 38.3, 40.1, 53.2, 70.3, and 76.7° correspond to Ti metal (Fig. 3(a)). The peaks at 39.8, 46.2, 68.1, and 82.02° correspond to the (111), (220), (200), and (311) phase of Pd, respectively (Fig. 3(b)). The average crystallite size of the Pd particles on TiO_2 was calculated using the Scherrer formula [30]. The results show that the particle size of the Pd is about 12 nm.

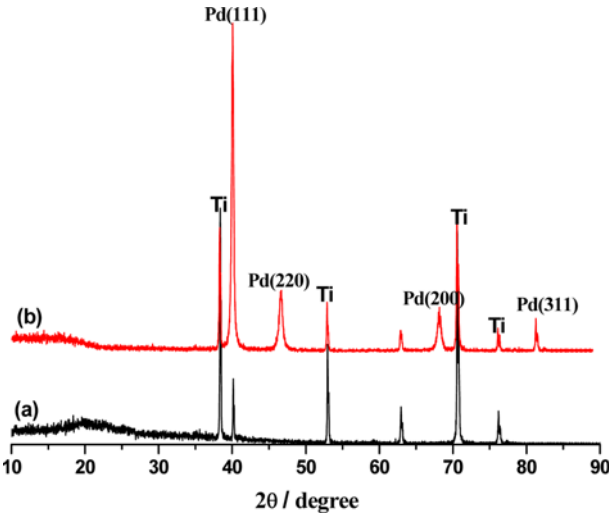

Fig. 3. XRD patterns of (a) TiO_2; and (b) the Pd/TiO_2 nanotube array electrodes.

The oxidation state of the Pd/TiO_2 interface was investigated by XPS (Fig. 4). The Ti($2p3/2$) spectrum shown in Fig. 4(a) is sharp and the obtained binding energy of 458.2 eV is typical for Ti^{4+}. The Pd($3d_{5/2}$) spectrum is shown in Fig. 4(b), and 336.12 eV is the binding energy obtained for Pd($3d_{5/2}$) in Pd^{2+} [31]. This is because of the higher Pd oxidation state on the surface. These higher oxidation states of Pd on the surface may be include PdOx.

2. HDH of 2, 4, 5-PCB at Pd/Ti and Pd/TiO_2 Nanotube Array Electrodes

Fig. 5 shows the HDH of 2,4,5-PCB at Pd/Ti and Pd/TiO_2 nanotube array electrodes under a constant potential of −1.0 V. They contained the same amount of Pd (1.8 mg/cm^2). The results indicate that the HDH of 2,4,5-PCB at Pd/TiO_2 was better than that at the Pd/Ti electrode. As shown in Fig. 5, within 180 min, 90% of the 2,4,5-PCB degraded and the yield of BP was 83% (current efficiency was 15%) over the Pd/TiO_2 nanotube array electrode. In contrast, only 68% of the 2,4,5-PCB degraded and the yield of BP was 59% at the Pd/Ti electrode.

The reason for the better activity of the Pd/TiO_2 nanotube array electrode compared with Pd/Ti is that a more uniform Pd particle size was dispersed on TiO_2 nanotube array electrode, and the size of Pd particles was smaller than that of Ti, as shown in the SEM in

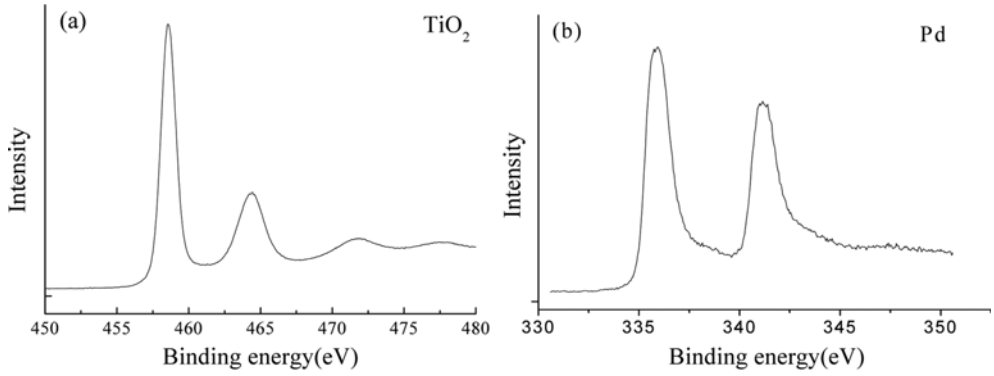

Fig. 4. XPS spectra showing (a) Ti 2p and (b) the Pd 3d binding energy region for the Pd/TiO_2 nanotube array electrodes.

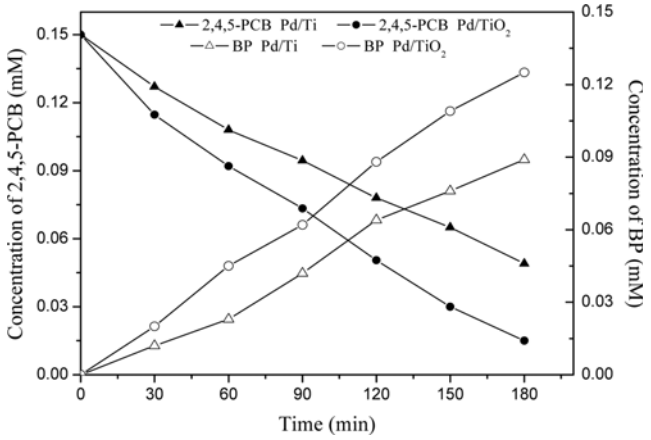

Fig. 5. HDH of 2,4,5-PCB at Pd/Ti and Pd/TiO_2 nanotube array electrodes (constant potential −1.0 V; Pd amount 1.8 mg/cm^2; catholyte 0.1 M CTAB with 40% MeOH; anolyte 0.2 M H_2SO_4).

Fig. 2. A smaller particle size results in a higher specific surface area of catalyst particles under the same amount of Pd, and thus the active sites are increased.

3. Influence of Cathode Potential

The cathode potential plays an important role in kinetic processes. As shown in Fig. 6, the HDH efficiency of 2,4,5-PCB increases significantly with an increase in potential from −0.6 V to −1.0 V, but a further increase in potential to −1.1 V the HDH of 2,4,5-PCB reduced. Under cathode potentials of −1.0 V and −1.1 V, the HDH efficiency of 2,4,5-PCB was 95% and 92%, respectively, and the current efficiency reached 13.3% and 10.9%, respectively.

These results are probably because due to the effect of cathode potential on the electrocatalytic HDH of 2,4,5-PCB. The increase the cathode potential increases the production of hydrogen atoms, which is advantageous in the electrocatalytic HDH. However, with an increase in the cathode potential, a number of side reactions such as hydrogen evolution occur, which is not favorable for the contact between 2,4,5-PCB and the electrode. This results in a decrease in the HDH of 2,4,5-PCB and the current efficiency. Similar results have been reported for the electrocatalytic HDH of PCB over a Pd/Ni electrode [32].

4. Influence of Catalyst Loading

Fig. 7 shows the concentration decay of 2,4,5-PCB vs. the reaction time when using a Pd/TiO_2 nanotube array electrode with different Pd loadings. Pd loading significantly affects the HDH. The

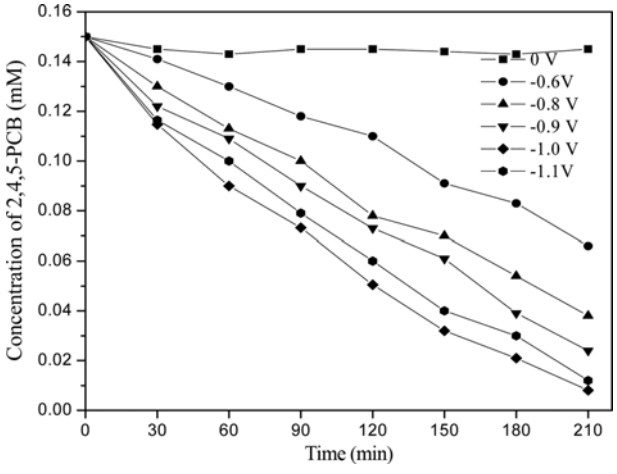

Fig. 6. Effect of cathode potential on the electrocatalytic HDH of 2,4,5-PCB (Pd amount 1.8 mg/cm^2; catholyte 0.1 M CTAB with 40% MeOH; anolyte 0.2 M H_2SO_4).

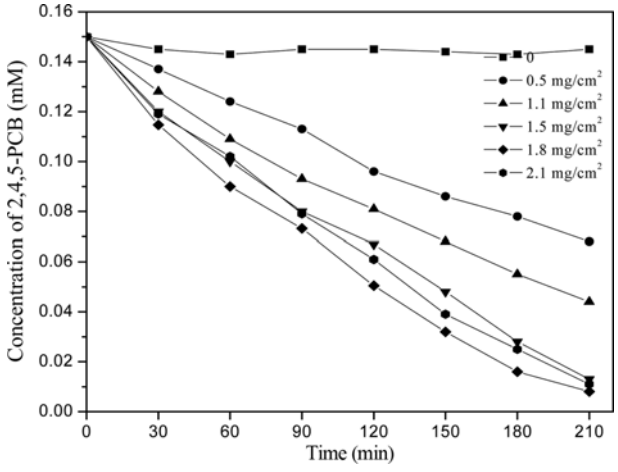

Fig. 7. Effect of Pd loading on the electrochemical HDH of 2,4,5-PCB (constant potential −1.0 V; catholyte 0.1 M CTAB with 40% MeOH; anolyte 0.2 M H_2SO_4).

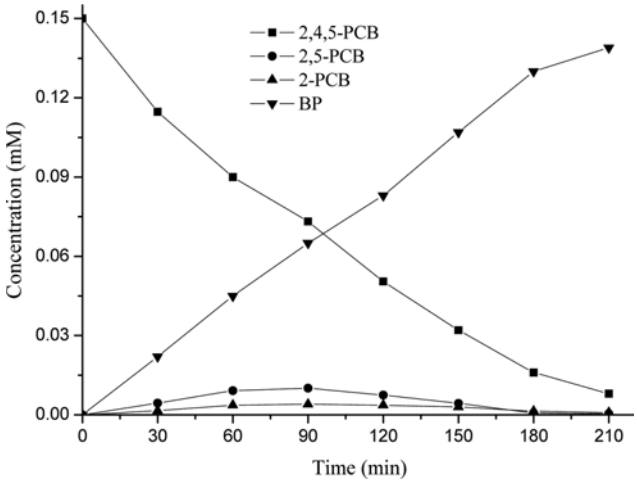

Fig. 8. Concentrations of the reactant and the products as a function of time during the HDH (constant potential −1.0 V; Pd amount 1.8 mg/cm^2; catholyte 0.1 M CTAB with 40% MeOH; anolyte 0.2 M H_2SO_4).

HDH activity of the Pd/TiO_2 nanotube array electrode increased sharply with an increase in Pd loading from 0.5 to 1.5 mg/cm^2 and it remained nearly constant with a further increase in Pd loading from 1.5 to 1.8 mg/cm^2. A further increase in catalyst loading resulted in a lower HDH.

These results prove that Pd provides catalytically active sites during the HDH of 2,4,5-PCB. Therefore, 2,4,5-PCB and active hydrogen can form a high concentration reaction phase on the surface of the Pd. An increase in Pd loading provides more catalytically active sites, which can accelerate the HDH of 2,4,5-PCB. However, with a high catalyst content, a reduction in catalyst dispersion leads to a reduced HDH reaction [24].

5. Intermediates and Products of 2,4,5-PCB

Fig. 8 shows the change in concentration of 2,4,5-PCB and the products formed during the HDH. As shown, the concentration of 2,4,5-PCB decreases rapidly from 1.5 mM to a concentration of less than 0.1 mM within 210 min of electrolysis. The HDH of 2,4,5-PCB gives biphenyl as the main product with a small amount of 2,5-DCB and 2-CB as transient partially dechlorinated intermediates. It is interesting that no 2,4-DCB, 3,4-PCB, 3-PCB, or 4-PCB was detected in the electrolyte solution. Therefore, the HDH of 2,4,5-PCB was selectively performed on the Pd/TiO_2 nanotube array electrode in this work. The results suggest that the reactivity of the chlorine at the 2-position in 2,4,5-PCB seems to be the lowest because of steric hindrance from the neighboring phenyl. Additionally, 2,5-DCB was found to be the major dechlorinated intermediate. This result indicates that the chlorine in the 4-position was more facile and thus more vulnerable to hydrogen attack than that in the 3-position. Additionally, the completely dechlorinated product (BP) was the main product from the early stage of the HDH of 2,4,5-PCB. These results imply that during the HDH of 2,4,5-PCB three chlorine atoms of 2,4,5-PCB were removed at the same stage before the desorption of the partially dechlorinated products into reaction solution. Therefore, the dechlorination pathways of 2,4,5-PCB at Pd/TiO_2 nanotube array electrode can be represented as Fig. 9.

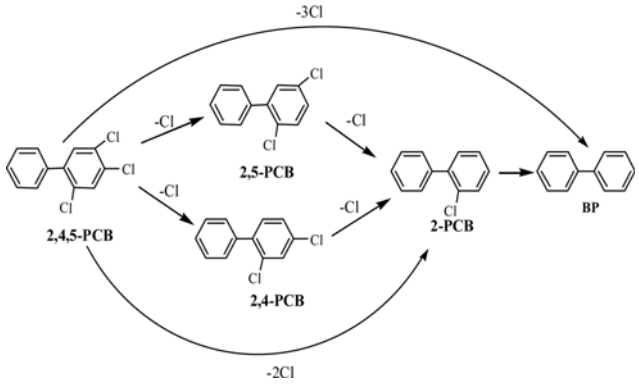

Fig. 9. Electrocatalytic HDH pathways of 2,4,5-PCB at Pd/TiO_2 nanotube array electrodes.

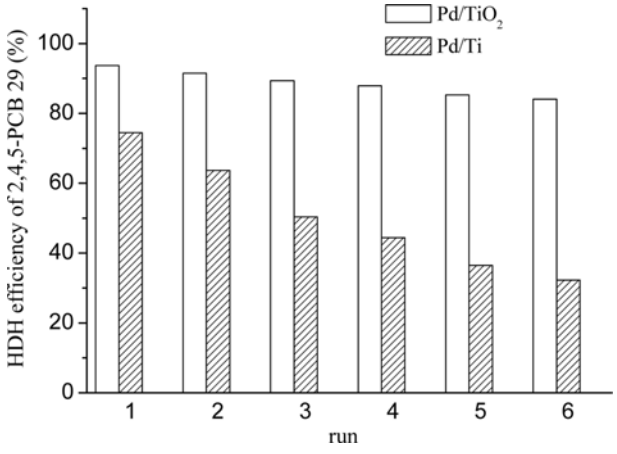

Fig. 10. Effect of electrode reuse on the HDH efficiency for 2,4,5-PCB at Pd/Ti and Pd/TiO_2 nanotube array electrodes (constant potential −1.0 V; Pd amount 1.8 mg/cm^2; catholyte 0.1 M CTAB with 40% MeOH, anolyte 0.2 M H_2SO_4; electrolysis 210 min).

6. Stability of the Electrode

The stability of the Pd/TiO_2 nanotube array electrode was compared to that of the Pd/Ti electrode. The correlation between the relative degree of HDH efficiency and the number of HDH reaction cycles is shown in Fig. 10. During each continuous HDH cycle, both the Pd/Ti and the Pd/TiO_2 nanotube array electrodes were deactivated. However, the results of six repeat experiments for the electrocatalytic HDH of 2,4,5-PCB over Pd/TiO_2 showed that the HDH efficiencies were high with a HDH efficiency of 84% (Fig. 10). In contrast, the HDH of 2,4,5-PCB decreased from 74% to 32% over Pd/Ti.

The loss of Pd should contribute to this marked decline in HDH efficiency. From the ICP-AES analysis, 5.5% of the initial amount of Pd leached from the Pd/TiO_2, and 20.6% leached from the Pd/Ti, respectively. These results imply that the Pd/TiO_2 nanotube array electrode has acceptable stability, which might be due to the compact interaction between the Pd particles and the TiO_2 nanotubes.

CONCLUSIONS

We report on the electrocatalytic HDH of PCB over palladized,

TiO_2 nanotube array electrode in an aqueous electrolyte. Well-aligned TiO_2 nanotube array structures were successfully fabricated by anodization on a Ti sheet, and Pd was loaded onto TiO_2 nanotubes by electrochemical deposition. The results show that the TiO_2 nanotube array electrode exhibits excellent properties, including a small particle size and good dispersion of the deposited Pd together with high chemical stability. These properties benefit the electrocatalytic HDH of PCB. Therefore, the Pd/TiO_2 nanotube array electrode exhibits better activity and stability toward the electrocatalytic HDH of PCB compared with the Pd/Ti electrode. Therefore, the TiO_2 nanotube array may be an acceptable candidate as an electrocatalyst support, because it possesses high electrocatalytic activity and acceptable chemical stability. This process has potential in the electrocatalytic HDH industry such as the detoxification of polychloroorganics in contaminated water.

ACKNOWLEDGEMENTS

The authors are grateful for financial support from the Nature Science Foundation of China (No. 20907025), and Yanhe Han is grateful for financial support from the Importation and Development of High-Caliber Talents Project of the Beijing Municipal Institutions (No. CIT&TCD201304098).

REFERENCES

1. S. Tanabe, *Environ. Pollut.*, **50**, 5 (1988).
2. D. Zacs, J. Rjabova and V. Bartkevics, *Environ. Sci. Technol.*, **47**, 9478 (2013).
3. C. Martinez, M. Canle, L. M. Fernandez, J. Santaballa and J. Faria, *Appl. Catal., B*, **107**, 110 (2011).
4. S. L. Gray, A. C. Shaw, A. X. Gagne and H. M. Chan, *J. Toxicol. Environ. Health, Part A*, **76**, 701 (2013).
5. T. Kishino and K. Kobayshi, *Water Res.*, **30**, 393 (1996).
6. S. Farwell, F. Beland and R. Geer, *J. Electroanal. Chem. Interfacial Electrochem.*, **61**, 303 (1975).
7. I. F. Cheng, Q. Fernando and N. Korte, *Environ. Sci. Technol.*, **31**, 1074 (1997).
8. R. Chetty, P. A. Christensen, B. T. Golding and K. Scott, *Appl. Catal., A*, **271**, 185 (2004).
9. P. Dabo, A. Cyr, F. Laplante, F. Jean, H. Ménard and J. Lessard, *Environ. Sci. Technol.*, **34**, 1265 (2000).
10. N. Ross, R. Spackman, M. Hitchman and P. White, *J. Appl. Electrochem.*, **27**, 51 (1997).
11. M. Higuera, M. Ruiz Montoya, R. Marín Galvín and J. Rodríguez Mellado, *J. Electroanal. Chem.*, **474**, 174 (1999).
12. G. Chen, Z. Y. Wang and D. G. Xia, *Electrochem. Commun.*, **6**, 268 (2004).
13. C. Durante, V. Perazzolo, L. Perini, M. Favaro, G. Granozzi and A. Gennaro, *Appl. Catal., B*, **158-159**, 286 (2014).
14. B. Z. Liu, X. B. Hu, Y. H. Deng, S. G. Yang and C. Sun, *J. Solid State Electrochem.*, **16**, 927 (2012).
15. C. Durante, B. Huang, A. A. Isse and A. Gennaro, *Appl. Catal., B*, **126**, 355 (2012).
16. B. Yang and G. Yu, *Environ. Sci. Technol.*, **41**, 7503 (2007).
17. H. Cheng, K. Scott and P. Christensen, *J. Electrochem. Soc.*, **150**, D25 (2003).
18. Z. R. Sun, X. F. Wei, X. Hu, K. Wang and H. T. Shen, *Colloids Surf., A: Physicochem. Eng. Aspects*, **414**, 314 (2012).
19. Z. Sun, H. Ge, X. Hu and Y. Peng, *Sep. Purif. Technol.*, **72**, 133 (2010).
20. Z. Sun, X. Wei, Y. Han, S. Tong and X. Hu, *J. Hazard. Mater.*, **244**, 287 (2013).
21. A. I. Tsyganok and K. Otsuka, *Appl. Catal., B*, **22**, 15 (1999).
22. L. Perini, C. Durante, M. Favaro, S. Agnoli, G. Granozzi and A. Gennaro, *Appl. Catal., B*, **144**, 300 (2013).
23. H. Cheng, K. Scott and P. Christensen, *J. Electrochem. Soc.*, **150**, D17 (2003).
24. C. Cui, X. Quan, H. Yu and Y. Han, *Appl. Catal., B*, **80**, 122 (2008).
25. C. Cui, X. Quan, S. Chen and H Zhao, *Sep. Purif. Technol.*, **47**, 73 (2005).
26. Y. Chen, H. Y. Li, W. J. Liu, Y Tu, Y. H. Zhang, W. Q. Han and L. J. Wang, *Chemosphere*, **113**, 48 (2014).
27. F. W. Wang, X. Y. Yan, M. Xu, S. D. Li and W. Y. Fang, *Electrochem. Acta*, **97**, 253 (2013).
28. Z. Ma, L. Zhang, R. Chen, W. Xing and N. Xu, *Chem. Eng. J.*, **138**, 517 (2008).
29. N. Lu, X. Quan, J. Li, S. Chen, H. Yu and G. Chen, *J. Phys. Chem. C*, **111**, 11836 (2007).
30. T. Arunagiri, T. D. Golden and O. Chyan, *Mater. Chem. Phys.*, **92**, 152 (2005).
31. H. Chen, Y. Shao, Z. Xu, H. Wan, Y. Wan, S. Zheng and D. Zhu, *Appl. Catal., B*, **105**, 255 (2011).
32. B. Yang, G. Yu and J. Huang, *Environ. Sci. Technol.*, **41**, 7503 (2007).